589

ntities is the

(14.58)

electrically torn antenna

and b. If the the Thévenin edance

(14.59)

'his Thévenin out resistance

(14.60)

the antenna, nat portion of resistance  $R_{ri}$ 

urrent  $I_{in}$  and

(14.61)

as

edance of an of an antenna. seen looking

$$\eta_r = \frac{P_{\text{rad}}}{P_{\text{in}}} = \frac{R_{ri}}{R_{ri} + R_L}$$
 (Dimensionless). (14.62)

Even though the input radiation resistance is a parameter that is measured in the near zone of an antenna, Equation (14.61) shows that it can be calculated by knowing only the far-zone radiation pattern. On the other hand, it is not so easy to calculate the input reactance  $X_{\rm in}$ . This is because  $X_{\rm in}$  represents energy stored in the fields close to the antenna. Hence,  $X_{\rm in}$  can only be calculated by first calculating the fields close to the antenna, which are typically much harder to calculate than the far-zone fields.

Another common resistance parameter used to describe antennas is the radiation resistance

$$R_{r} = \frac{2P_{\rm rad}}{I_{\rm max}^2}$$
 [\Omega], (14.63)

where  $I_{\max}$  is the maximum current on the antenna. This resistance is related to the input radiation resistance  $R_{ri}$ , but they are equal only when the maximum current on the antenna appears at the input terminals. In general,  $R_{ri}$  and  $R_r$  are related by

$$R_{ri} = \left[\frac{I_{\text{max}}}{I_{\text{in}}}\right]^2 R_r. \tag{14.64}$$

## 14-5 Simple Antennas

Simple antennas consist of a single radiating element or structure. The major classes of simple antennas include straight wire antennas, loop antennas, aperture antennas, and reflector antennas. These antennas are often used individually, but they can also be used as the basic building blocks of larger antenna structures called arrays. In this section, we will outline the basic characteristics of the major classes of simple antennas. Later, we will discuss how these elements can be arranged to form arrays.

## 14-5-1 DIPOLES

We have already discussed one type of dipole, the infinitesimal (or short) dipole. This antenna is simple to model, but is not very practical for a number of reasons, the most important being that its input impedance is undesirable—a small resistance in series with a very large capacitive reactance. Because of this, it is very difficult to design efficient matching networks that allow short dipoles to be driven by amplifying circuits. However, when the dipole length is on the order of a half wavelength or more, its input impedance becomes much more attractive. This, along with its mechanical simplicity, makes the finite-length dipole attractive for a number of applications.

In order to determine the fields generated by finite-length dipoles, we must first determine what kinds of current distributions are excited on these wires by a voltage feed. Calculating these currents directly from Maxwell's equations is a difficult problem, since both the currents and the fields must be found simultaneously. A simpler, alternative procedure is to consider the wire configurations shown in Figure 14-10.

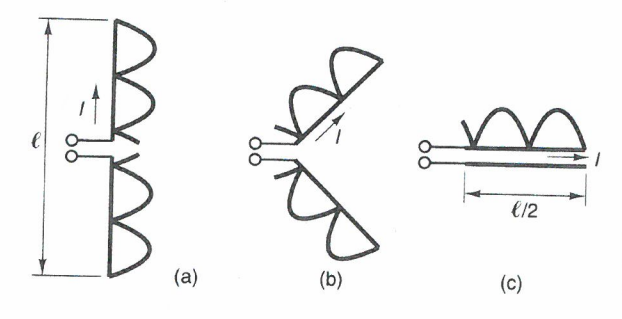


Figure 14-10 Sequence of wire configurations for determining the current distributions on dipoles: a) A straight dipole. b) A slightly bent dipole. c) An open-circuited transmission line.

In Figure 14-10a, a dipole antenna of length  $\ell$  is fed at its center by a voltage source. Figures 14-10b and c show the same geometry, but with the dipole arms bent progressively towards each other until they are parallel. At the end of this progression, the wires form a uniform, open-circuited transmission line. Even though the properties of transmission lines and antennas are quite different, the current on the wires remains remarkably constant throughout the progression. This means that we can use the transmission-line current as an approximation of the antenna current. Using standard transmission-line analysis, we find that the current on the upper wire of Figure 14-10c is of the form

$$I(z) = I_{\rm m} \sin \left[ k \left( \frac{\ell}{2} - z \right) \right],$$

where  $k=\omega\sqrt{\mu_o\epsilon_o}$  is the phase constant of a transmission line with an air dielectric and z=0 occurs at the terminals. Since the currents on the upper and lower wires have even symmetry, the preceding expression for I(z) can be used over the entire length of the dipole in Figure 14-10a by replacing z with |z|, yielding

$$I(z) = I_m \sin\left[k\left(\frac{\ell}{2} - |z|\right)\right]. \tag{14.65}$$

This approximation for I(z) is most accurate when the dipole is fed at its center, but can also be used for off-center-fed dipoles.

Figures 14-11a-c show the current distributions excited on dipoles of three different lengths.

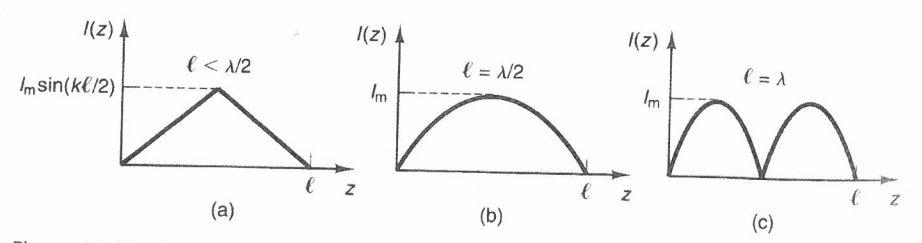


Figure 14-11 Current distributions on dipole antennas: a)  $\ell \ll \lambda/2$ . b)  $\ell = \lambda/2$ . c)  $\ell = \lambda$ .

591

As can be seen, when  $\ell \ll \lambda/2$ , the shape of the current is roughly triangular. For longer lengths, I(z) takes on a sinusoidal shape, with more lobes on longer length wires. For all lengths, the current  $I_0$  at the center of the wire is given by  $I_0 = I_m$ . Having found an expression for the distance of half wavelengths,  $I_0 = I_m$ .

Having found an expression for the dipole current I(z), we can calculate the total radiated field by summing the contributions from each infinitesimal segment along the dipole. Referring to Figure 14-12 and using the field of an infinitesimal current segment (Equation (14.41)), we can write the far-zone contribution from the segment at  $z=z^{\prime}$  as

$$\mathbf{dE} = \frac{jkI(z')dz'}{4\pi} \, \eta \sin \theta' \, \frac{e^{-jkR}}{R} \, \hat{\mathbf{a}}_{\theta}, \tag{14.66}$$

where R is the length of a line from the segment to the observer and  $\theta'$  is the angle that this line makes with the z-axis. When  $r \gg \ell/2$ , all lines drawn from the wire to the observer are nearly parallel, so  $\theta \approx \theta'$  and

$$R \approx r - z' \cos \theta, \tag{14.67}$$

where r and  $\theta$  are the position coordinates of the observer. Substituting Equation (14.67) into Equation (14.66) yields

$$\mathbf{dE} = \frac{jkI(z')e^{-jkr}dz'}{4\pi r}\eta\sin\theta\,\,\hat{\mathbf{a}}_{\theta}e^{jkz'\cos\theta}.\tag{14.68}$$

Replacing I(z') with  $I_m \sin\{k[(\ell/2) - |z|]\}$  and integrating all the contributions to the field along the wire, we obtain

$$\mathbf{E} = \int_{\text{BOTTOM}}^{\text{TOP}} \mathbf{dE} = \frac{jkI_m e^{-jkr}}{4\pi r} \, \eta \sin \theta \, \hat{\mathbf{a}}_{\theta} \int_{-\ell/2}^{\ell/2} \sin \left[ k \left( \frac{\ell}{2} - |z| \right) \right] e^{jkz' \cos \theta} dz'.$$

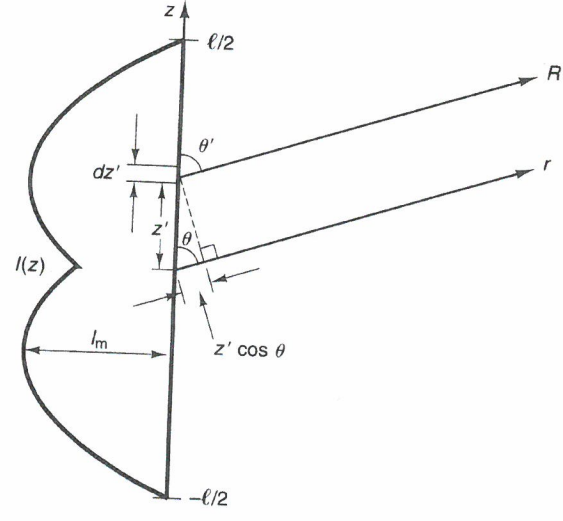


Figure 14-12 Geometry for determining the far-zone radiated field of a finite-length dipole.

he current aight e. c) An

ge source. t progression, the perties of s remains n use the g standard are 14-10c

dielectric wer wires the entire

(14.65)

enter, but

three dif-



c)  $\ell = \lambda$ .

Using Euler's identity to expand the exponential term and evaluating the resulting integral, we get

$$\mathbf{E} = \frac{j\eta I_m e^{-jkr}}{2\pi r} F(\theta) \,\hat{\mathbf{a}}_{\theta} \qquad [\text{V/m}], \tag{14.69}$$

where  $F(\theta)$  is called the *pattern function* and is given by

$$F(\theta) = \frac{\cos\left(\frac{k\ell}{2}\cos\theta\right) - \cos\frac{k\ell}{2}}{\sin\theta}.$$
 (14.70)

Since in the far zone  ${\bf E}$  and  ${\bf H}$  behave locally as plane waves, we also have  $H_\phi=E_\theta/\eta$ . Hence,

$$\mathbf{H} = \frac{jI_m e^{-jkr}}{2\pi r} F(\theta) \,\hat{\mathbf{a}}_{\phi}. \tag{14.71}$$

Figure 14-13 shows the pattern functions for four different-length wire antennas, each normalized to a maximum amplitude of unity. As can be seen, dipole pattern functions become more complex as their lengths increase. The reason for this is that the phase difference between the fields emanating from the endpoints of the dipole becomes more pronounced as the dipole length increases. At  $\theta=90^{\circ}$ , all delays are

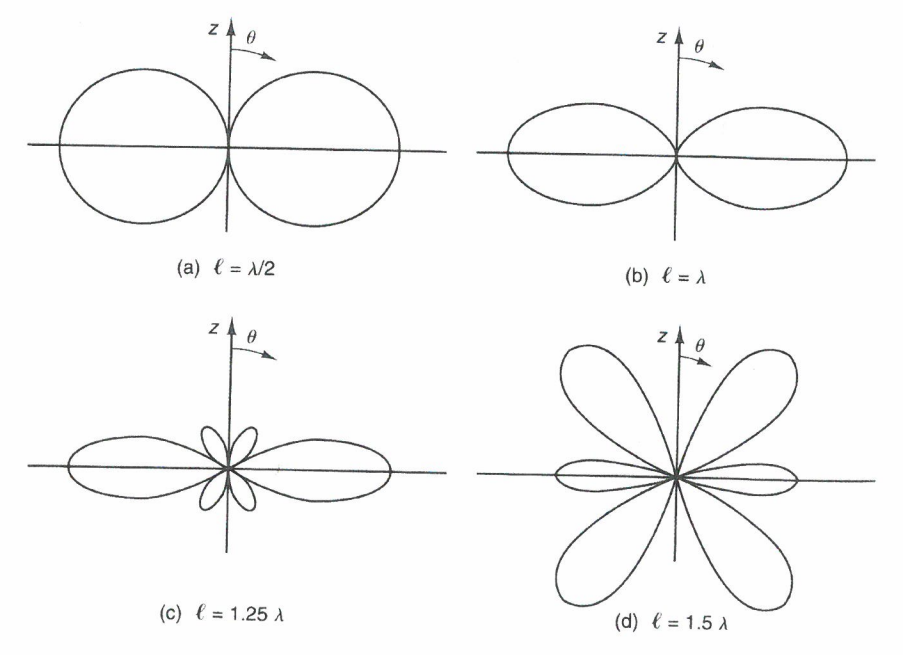


Figure 14-13 Pattern functions for dipole antennas oriented along the z-axis: a)  $\ell = \lambda/2$ . b)  $\ell = \lambda$ . c)  $\ell = 1.25\lambda$ . d)  $\ell = 1.5\lambda$ .

D

593

e resulting

(14.69)

(14.70)

$$H_{\phi} = E_{\theta}/\eta$$
.

(14.71)

e antennas, ole pattern this is that the dipole l delays are



) >---

a) 
$$\ell = \lambda/2$$
.

equal, since the current lies along the z-axis. But as  $\theta$  approaches  $0^{\circ}$  or  $180^{\circ}$ , contributions from the different points on the dipole arrive with significant phase differences.

We can find the power radiated by a wire antenna by integrating the radiation intensity over a large sphere that surrounds the wire. Substituting Equations (14.69) and (14.70) into Equation (14.51), we see that the radiation intensity is

$$U(\theta,\phi) = \frac{\eta I_m^2}{8\pi^2} F^2(\theta).$$

Substituting  $U(\theta, \phi)$  into Equation (14.55), we find that the directivity  $D_o$  is given by

$$D_{o} = \frac{U_{\text{max}}}{U_{\text{ave}}} = \frac{F^{2}(\theta)\big|_{\text{max}}}{\frac{1}{4\pi} \int_{0}^{2\pi} \int_{0}^{\pi} F^{2}(\theta) \sin \theta \, d\theta \, d\phi} = \frac{F^{2}(\theta)\big|_{\text{max}}}{\frac{1}{2} \int_{0}^{\pi} F^{2}(\theta) \sin \theta \, d\theta}.$$

The integral in this expression cannot be evaluated in closed form, but it can be manipulated into a form that contains well-tabulated functions,<sup>4</sup> or it can be evaluated numerically. Figure 14-14 show  $D_o$  as a function of  $\ell/\lambda$ . As can be seen,  $D_o \approx 1.5$  when  $\ell \ll \lambda/2$ . For  $\ell = \lambda/2$ , the directivity is

$$D_o = 1.64 = 2.15 \text{ [dB]}$$
 (Half wave dipole). (14.72)

Remembering that the current at the dipole center is  $I_{\rm in} = I_m \sin{(k \ell/2)}$ , we can determine the input radiation resistance of a lossless, center-fed dipole using Equation (14.61):

$$R_{\rm in} = R_{ri} = \frac{2P_{\rm rad}}{I_{\rm in}^2} = \frac{\eta}{2\pi \sin^2(k\,\ell/2)} \int_0^{\pi} F^2(\theta) \sin\theta \, d\theta. \tag{14.73}$$

The dark curve in Figure 14-15 is a plot of  $R_{\rm in}$  as a function of dipole length. The values in this curve were obtained using Equation (14.73), except for the lengths in the range  $0.8\lambda$  to  $1.0\lambda$ , where Equation (14.73) predicts unreasonably large values. These incorrect values occur because the approximate current distribution goes to zero for this range of dipole lengths, whereas the actual current distribution does not. To

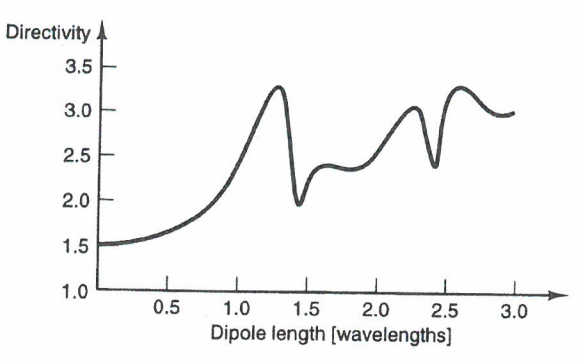


Figure 14-14 Dipole directivity vs. length in wavelengths.

<sup>&</sup>lt;sup>4</sup> See C. Balanis, Antenna Theory (Harper & Row publishers). New York, 1982.

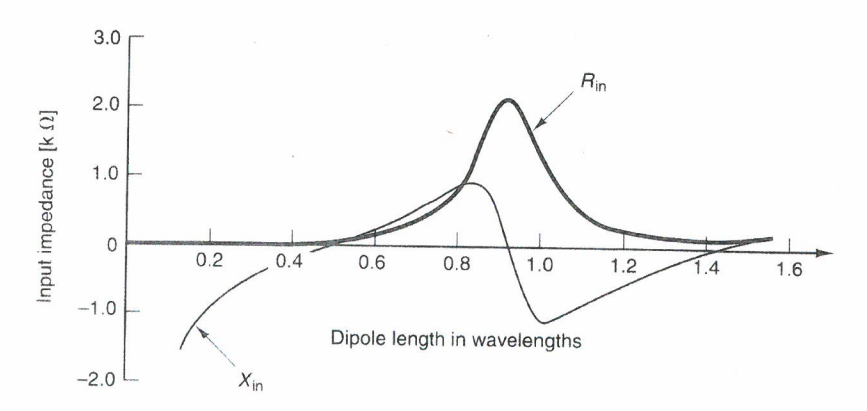


Figure 14-15 Input resistance and reactance of a center-fed dipole vs. length.

account for that behavior, the values of  $R_{\rm in}$  plotted in the aforesaid range were obtained using an advanced numerical technique that calculates the exact current distribution on the wire. The figure also shows the values of the input reactance  $X_{\rm in}$ , which were obtained using the same numerical technique throughout the entire range of dipole lengths.

As can be seen from Figure 14-15, the input impedance of a center-fed dipole is purely resistive for certain lengths, called *resonant lengths*. The shortest resonant length is  $\ell \approx \lambda/2$  ( $\ell = 0.475\lambda$ , to be more exact), for which we obtain

$$Z_{\rm in} \approx 73 + j \, 0 \quad [\Omega]$$
 (Half wave dipole). (14.74)

There are other resonant lengths, but the half-wave dipole is by far the most popular choice, since it has the shortest length, the simplest radiation pattern, and a relatively large bandwidth over which  $Im(Z_{in})$  is small.

Dipole antennas were among the first antennas used in electrical communications and are still used in a wide range of applications. They are particularly popular at RF frequencies, where wavelengths are long. This is because it is usually much easier to mount a long wire between towers and trees than it is to position a large metal surface, such as a reflector.

There are times when dipoles are formed unintentionally. For instance, coaxial cables act as dipole radiators when they carry unbalanced currents. As we discussed in Section 9-3-7, a nonzero magnetic field is generated outside a coaxial cable that has unbalanced currents. When the currents and fields are time varying, a time-varying electric field is also produced, since time-varying electric fields always accompany time-varying magnetic fields. Thus, to an outside observer, the cable appears to be a thick wire dipole carrying the common-mode current (i.e., the sum of the inner and outer currents).

Radiation from cables is a significant problem in digital equipment, since it causes interference with communication services (such as radio and television) and can also interfere with the operation of the digital systems themselves. A common way of suppressing this radiation is to wrap an offending cable around a ferrite core, as shown in Figure 9-26b, which reduces the common-mode current.

Two types of wire antennas that are closely related to dipoles are monopoles and folded dipoles, which we will discuss in the paragraphs that follow.

**Monopole Antennas.** Figure 14-16a shows a monopole antenna, consisting of a straight wire, mounted perpendicular to a conducting ground plane and fed with a voltage  $V_{\rm in}$  at the base. At first look, this antenna may appear to have little relation to the dipole, since currents flow on both the wire and the ground plane. However, we can determine the fields of a monopole by using the equivalent geometry shown in Figure 14-16b. Here, the ground plane is replaced by an image wire that carries a current which is a mirror image of the monopole current. To ensure that the current on the equivalent dipole has the required even symmetry, a voltage  $V_{\rm in}$  is applied symmetrically, just below the z=0 plane. The fields above the z=0 plane are unchanged, since the  $E_{\rm tan}=0$  boundary condition once imposed by the ground plane is now maintained by the image currents. As a result, the radiation pattern of a monopole is identical to a dipole whose length is exactly twice that of the monopole.

We can find the input impedance of a monopole using the equivalent dipole shown in Figure 14-16b. Starting with  $Z_{\rm in}=V_{\rm in}/I_{\rm in}$ , we can rewrite this as

Figure 14-16 A monopole over a conducting plane and its equivalent dipole.

a) The monopole and ground plane. b) The equivalent dipole in free space.

1.6

th.

rere obtained stribution on , which were age of dipole

-fed dipole is test resonant

(14.74)

most popular d a relatively

nmunications opular at RF such easier to netal surface,

tance, coaxial e discussed in able that has time-varying s accompany pears to be a the inner and

$$Z_{\text{monopole}} = \frac{V_{\text{in}}}{I_{\text{in}}} = \frac{1}{2} \frac{2V_{\text{in}}}{I_{\text{in}}}.$$

Since the two series voltage sources in the equivalent dipole constitute a single voltage of value  $2V_{\rm in}$ , it follows that  $2V_{\rm in}/I_{\rm in}$  is the impedance of the equivalent dipole. Thus, the monopole input impedance is given by

$$Z_{\text{monopole}} = \frac{1}{2} Z_{\text{dipole}}.$$
 (14.75)

For a monopole of length  $\ell \approx \lambda/4$ , we have

$$Z_{\text{monopole}} = \frac{1}{2} \times 73 = 36.5 \quad [\Omega] \quad (\lambda/4 \text{ monopole}).$$
 (14.76)

Because monopole antennas require only half the wire length of dipole antennas, they are often used in low-frequency systems, where wavelengths are long. They also have radiation patterns that are ideal for ground-to-ground communication systems, since the direction of maximum radiation is parallel to the ground. Also, unlike horizontal dipoles, which must be mounted several wavelengths above the ground to be effective (due to reflections off the ground that tend to cancel the fields), monopoles work best when mounted directly above the ground.

**Folded Dipoles.** Another common variation of the dipole wire antenna is the folded dipole, shown in Figure 14-17a. As can be seen, this antenna consists of two  $\lambda/2$  dipoles connected in parallel, with the feed point at the center of one of the dipoles. Although at first glance it may appear that a folded dipole antenna will act more as a loop antenna than as a dipole, the small area enclosed by the wires prevents it from acting in the loop mode.

Folded dipoles can be analyzed quite easily by recognizing that, according to the superposition principle, the single voltage feed can be represented as the sum of the

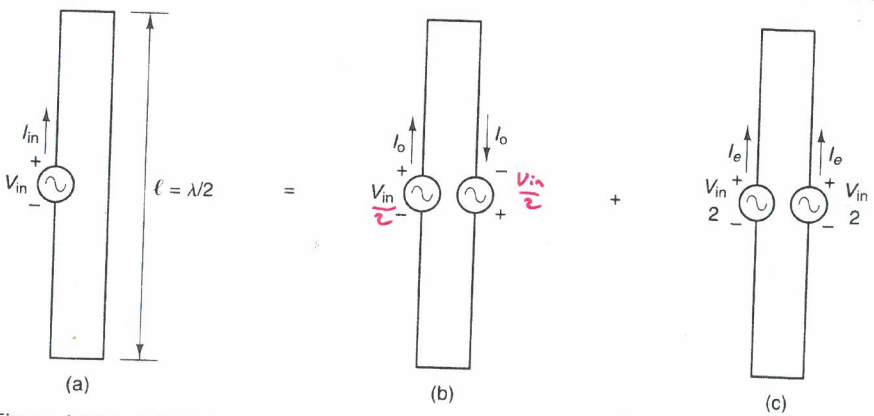


Figure 14-17 A folded dipole and its odd and even components. a) A folded dipole, fed at a single port. b) The odd-mode excitation. c) The even-mode excitation.